Published in final edited form as:
J Am Chem Soc. 2018 December 12; 140(49): 17071–17078. doi:10.1021/jacs.8b08704.

Rapid Dissolution of $BaSO_4$ by Macropa, an Eighteen-Membered Macrocycle with High Affinity for Ba^{2+}

Nikki A. Thiele, **Samantha N. MacMillan**, and **Justin J. Wilson***
Department of Chemistry and Chemical Biology, Baker Laboratory, Cornell University, Ithaca, New York 14853, USA

Abstract

Insoluble $BaSO_4$ scale is a costly and time-consuming problem in the petroleum industry. Clearance of $BaSO_4$-impeded pipelines requires chelating agents that can efficiently bind Ba^{2+}, the largest non-radioactive +2 metal ion. Due to the poor affinity of currently available chelating agents for Ba^{2+}, however, the dissolution of $BaSO_4$ remains inefficient, requiring very basic solutions of ligands. In this study, we investigated three diaza-18-crown-6 macrocycles bearing different pendent arms for the chelation of Ba^{2+} and assessed their potential for dissolving $BaSO_4$ scale. Remarkably, the bis-picolinate ligand macropa exhibits the highest affinity reported to date for Ba^{2+} at pH 7.4 (log K' = 10.74), forming a complex of significant kinetic stability with this large metal ion. Furthermore, the $BaSO_4$-dissolution properties of this ligand dramatically surpass those of the state-of-the-art ligands DTPA and DOTA. Using macropa, complete dissolution of a molar equivalent of $BaSO_4$ is reached within 30 min at RT in pH 8 buffer, conditions under which DTPA and DOTA only achieve 40% dissolution of $BaSO_4$. When further applied for the dissolution of natural barite samples, macropa also outperforms DTPA, showing that this ligand is potentially valuable for industrial processes. Collectively, this work demonstrates that macropa is a highly effective chelator for Ba^{2+} that can be applied for the remediation of $BaSO_4$ scale.

Graphical Abstract

***Corresponding Author** jjw275@cornell.edu.

N.A.T. and J.J.W. have filed a provisional patent on the application of this class of ligands for $BaSO_4$ scale dissolution.

ASSOCIATED CONTENT
Supporting Information.
Experimental details, compound characterization, and supporting figures and tables (PDF)
Crystallographic information files (PDF)
This material is available free of charge via the Internet at http://pubs.acs.org.

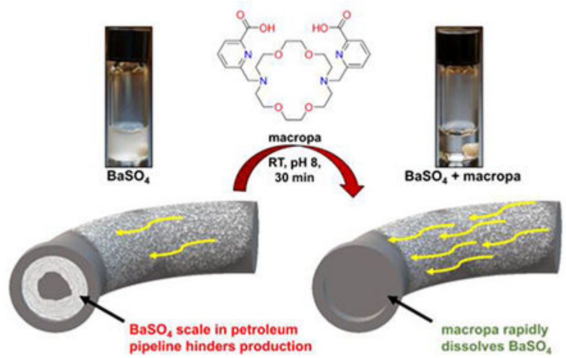

Introduction

Barium, the 14th most abundant element in the Earth's crust, is the heaviest and largest non-radioactive alkaline earth (AE) metal.[1,2] Administered as a suspension of $BaSO_4$, this element has been employed for over a century as a contrast agent for X-ray imaging of the gastrointestinal tract.[3] The insolubility of $BaSO_4$ ($K_{sp} = 1.08 \times 10^{-10}$)[4] is essential for its use in medicine because it prevents this toxic heavy metal from being absorbed into the body. This same physical property, however, presents a serious problem in the industrial sector. Precipitation of $BaSO_4$ occurs frequently in oil field and gas production operations. When Ba^{2+}-rich formation waters mix with SO_4^{2-}-rich seawater, an intractable scale of $BaSO_4$ is deposited, obstructing downhole pipes and surface equipment.[5] As such, $BaSO_4$ scale is a major economic burden to the petroleum industry that slows or halts production and requires costly scale removal efforts.[6,7] In addition, the scale poses a significant health hazard to petroleum workers. Naturally occurring radioactive material (NORM), particularly long-lived bone-seeking Ra^{2+} ions, is readily incorporated into $BaSO_4$ and is mobilized during scale remediation, exposing humans to toxic levels of radioactivity.[8,9] Hence, the efficient and safe removal of $BaSO_4$ scale is of global significance.

The elimination of $BaSO_4$ scale is achieved by solubilization using chelating agents.[10–14] One of the most commonly used chelators is the acyclic ligand DTPA (Chart 1).[12] The thermodynamic stabilities of DTPA complexes of the AEs, however, decrease with increasing ionic radius of the metal ion, rendering DTPA a low-affinity ligand for Ba^{2+} ($\log K_{BaL} = 8.78$).[15] Extreme conditions of high pH (pH > 11) and heat are required to efficiently remove scale using DTPA,[16–18] reflecting the fact that this ligand is not optimal for the chelation of Ba^{2+}. The tetraaza macrocycle DOTA (Chart 1) has also been investigated for the dissolution of $BaSO_4$.[12] Despite having the highest reported thermodynamic affinity for Ba^{2+} in aqueous solution ($\log K_{BaL} = 11.75$),[19–21] DOTA dissolves $BaSO_4$ less efficiently than DTPA,[22] reflecting the slow metal-binding kinetics of this macrocycle. Collectively, these limitations underscore the need to develop new ligands for Ba^{2+}.

Despite the need for new, more effective Ba^{2+} chelators for the removal of $BaSO_4$ scale, few efforts to date have been directed towards this objective. The development of improved chelators for Ba^{2+} has further been hindered by the lack of fundamental coordination chemistry studies of this ion.[23] A key challenge for the chelation of Ba^{2+} arises from the fact that the large AEs engage primarily in ionic, rather than covalent, binding interactions with ligands. The strength of these ionic bonds is proportional to the charge-to-size ratio of the metal center, with smaller ratios giving rise to weaker electrostatic interactions. As the largest non-radioactive +2 ion in the Periodic Table (IR = 1.35 Å, CN6),[2] Ba^{2+} has a low charge density, resulting in coordination complexes of lower stability compared to the smaller AEs. As a result, the selective, rapid, and stable chelation of Ba^{2+} has remained elusive.

Based on our success in using the expanded 18-membered macrocycle macropa (Chart 1) for the chelation of the largest +3 ion, actinium (IR = 1.12 Å, CN6),[24–26] we investigated the suitability of this ligand for the large Ba^{2+} ion. Additionally, two novel ligands, macropaquin and macroquin–SO_3 (Chart 1), were evaluated to systematically probe the influence of varying the metal-binding pendent arms on Ba^{2+} coordination. Our studies show that macropa has the highest affinity for Ba^{2+} at pH 7.4 reported to date, to the best of our knowledge. This ligand also possesses excellent selectivity for large over small AEs, a feature that is not observed for conventional ligands such as DTPA and DOTA. Furthermore, macropa exhibits superior $BaSO_4$-dissolution properties relative to DTPA and DOTA, rapidly solubilizing $BaSO_4$ under mild conditions. These results reveal macropa to be an exceptional chelator for the large Ba^{2+} ion and establish proof of concept for its industrial application as a scale dissolver, demonstrating that fundamental coordination chemistry principles can be applied to satisfy unmet societal needs.

Results and Discussion

Previous studies have shown that macropa selectively binds large over small metal ions;[24,27,28] notably, the affinity of macropa for Sr^{2+} ($\log K_{SrL} = 9.57$) is 4 orders of magnitude higher than for the smaller Ca^{2+} ion ($\log K_{CaL} = 5.25$).[29] Based on these findings, we hypothesized that macropa may possess even higher affinity for Ba^{2+}. Macroquin, a ligand in which the picolinate pendent arms of macropa are replaced with 8-hydroxyquinoline groups, has also been investigated.[30] Ligands of this class are highly selective for Ba^{2+} over smaller AEs, although this selectivity has only been demonstrated in organic solvents owing to the poor aqueous solubility of these ligands.[30–32] To increase aqueous solubility, we installed sulfonate groups onto the 8-hydroxyquinoline arms of the macrocycle, generating macroquin–SO_3. Finally, to investigate potential metal-binding synergy between the two types of pendent arms, the mixed variant, macropaquin, was synthesized by the stepwise installation of one picolinate group and one 8-hydroxyquinoline group onto the diaza-18-crown-6 backbone. Details of the synthesis and characterization of the ligands are provided in the Supporting Information, SI (Figures S1–S4, S9–S12).

To probe the fundamental coordination chemistry of these ligands with Ba^{2+}, their complexes with this ion were prepared (Figures S5–S8, S13, S14) and analyzed by X-ray crystallography to elucidate their solid-state structures (Figure 1, Tables S1–S4). In each complex, the Ba^{2+} ion is situated slightly above the diaza-18-crown-6 ring, and the two pendent arms are oriented on the same side of the macrocycle. The coordination sphere of the Ba^{2+} ion comprises all ten donor atoms of each ligand (N_4O_6), together with an oxygen atom from a coordinated solvent molecule that penetrates each macrocycle from the opposite face. Similar 11-coordinate arrangements were observed for the Ba^{2+} complexes of BHEE-18-aneN_2O_4, a diaza-18-crown-6 macrocycle bearing two pendent –$CH_2CH_2OCH_2CH_2OH$ arms,[33,34] and macroquin–Cl, in which the sulfonate groups of macroquin–SO_3 are replaced by chlorine atoms.[31]

The ligand conformation, which can be denoted with Δ or Λ to indicate the pendent arm helical twist and δ or λ to indicate the tilt of each five-membered chelate ring,[35] is identical for the three complexes. Each ligand attains the Δ(δλδ)(δλδ) conformation, present in equal amounts with its enantiomer. For complexes of macropa with other large metal ions, this conformation is also the most stable.[27,29] Protonation of one picolinate arm of macropa and the 8-hydroxyquinoline arm of macropaquin gives rise to complexes of the cationic formulae $[Ba(Hmacropa)(DMF)]^+$ and $[Ba(Hmacropaquin)(DMF)]^+$, respectively. By contrast, macroquin–SO_3 forms a neutral complex with Ba^{2+}, $[Ba(H_2macroquin–SO_3)(H_2O)]$. In this case, both phenolates are protonated to form neutral donors, but the sulfonic acid groups exist in the deprotonated anionic form. As reflected by the similar distances between Ba^{2+} and the two nitrogen atoms of each macrocycle, the Ba^{2+} ion is situated symmetrically within the macrocycle of each complex. Collectively, the structural features of these complexes suggest that macropa, macropaquin, and macroquin–SO_3 can optimally accommodate the large Ba^{2+} ion.

To further evaluate the coordination properties of the ligands with the AEs, their protonation constants and the stability constants of their Ca^{2+}, Sr^{2+}, and Ba^{2+} complexes were measured by potentiometric titration in 0.1 M KCl (Table 1, Figures S15–S17). For comparison, corresponding values for DTPA and DOTA, the current state of the art for Ba^{2+} chelation, are also provided. The protonation constants of the ligands are defined in Eq. 1. The stability constants and protonation constants of the metal complexes are expressed in Eqs. 2 and 3, respectively.

$$K_{ai} = \frac{[H_iL]}{[H_{i-1}L][H^+]} \quad (1)$$

$$K_{ML} = \frac{[ML]}{[M][L]} \quad (2)$$

$$K_{MH_iL} = \frac{[MH_iL]}{[MH_{i-1}L][H^+]} \quad (3)$$

A comparison of the ligand protonation constants reveals that sequential replacement of each picolinate arm of macropa by 8-hydroxyquinoline-based binding groups significantly decreases the basicity of the nitrogen atoms of the macrocyclic core to which they are attached. This trend is evidenced by the lower amine protonation constants of 7.15 (log K_{a2})

and 6.97 (log K_{a3}) for macropaquin and 6.75 (log K_{a3}) and 6.62 (log K_{a4}) for macroquin–SO_3, versus 7.41 (log K_{a1}) and 6.899 (log K_{a2}) for macropa. A comparison between related ethylenediamine-derived ligands bearing either picolinate or 8-hydroxyquinoline groups also shows that the basicity of the secondary amines is lower when attached to the latter.[36,37] The electron-withdrawing sulfonate groups on macroquin–SO_3 give rise to more acidic phenols (log K_{a1} = 9.34, log K_{a2} = 9.43) compared to macropaquin (log K_{a1} = 10.33). Notably, the second protonation constant of macroquin–SO_3 is slightly larger than the first protonation constant. This apparent reversal in expected values may be attributed to intramolecular hydrogen bonding that slightly stabilizes the second proton; upon its removal, the hydrogen bond network is broken, and the final remaining proton becomes more acidic. This phenomenon has been previously reported for other macrocyclic ligands.[38,39]

Because protons compete with metal ions for binding sites on ligands, ligand basicity is an important factor that contributes to the affinity of a ligand for a metal ion at a specific pH.[40,41] The overall basicity of the ligands, taken as the sum of their log K_a values, follows the order macropa (19.99) < macropaquin (27.69) < macroquin–SO_3 (32.14). The speciation of the ligands reflects these overall basicity values. At pH 7.4, 43% of macropa is fully deprotonated (L^{2-}), consistent with the low overall basicity of this ligand (Figure S18). By contrast, fully deprotonated macropaquin^{2-} and macroquin–SO_3^{4-} do not exist in solution below pH 8 (Figures S19 and S20). At pH 7.4, the monoprotonated species of macropaquin, HL^-, predominates (56%), whereas macroquin–SO_3 is mostly present as H_2L^{2-} (78%). On the basis of these results, macropaquin and macroquin–SO_3 may chelate metal ions less effectively than macropa near neutral pH due to greater competition with protons for binding.

With the protonation constants in hand, the stability constants of these ligands with Ca^{2+}, Sr^{2+}, and Ba^{2+} were determined. Remarkably, macropa, macropaquin, and macroquin–SO_3 all exhibit significant thermodynamic preferences for large over small AEs; the measured log K_{ML} values are highest for complexes of Ba^{2+} and lowest for complexes of Ca^{2+}. However, the affinities of the ligands for Ba^{2+} and Sr^{2+} decrease as the picolinate arms on the macrocyclic scaffold are replaced with 8-hydroxyquinoline or 8-hydroxyquinoline-5-sulfonic acid arms. For example, log K_{BaL} values of 11.11, 10.87, and 10.44 were measured for complexes of macropa, macropaquin, and macroquin–SO_3, respectively, containing zero, one, and two 8-hydroxyquinoline-based pendent arms. This trend signifies that 8-hydroxyquinoline-based pendent arms may not be suitable metal-binding groups for the chelation of large metal ions such as Ba^{2+}.

Refinement of our potentiometric titration data also revealed the presence of protonated metal complexes, or MHL and MH_2L species, for all three ligands bound to Ca^{2+}, Sr^{2+}, and Ba^{2+} (Figures 2 and S21–26). The inclusion of these species within our solution phase model is consistent with the results from X-ray crystallography, which also identified these species in the solid state (Figure 1). The speciation diagrams for solutions of Ba^{2+} and the three ligands, based on the thermodynamic constants in Table 1, are shown in Figure 2. The major species present at pH 7.4 is the ML species for macropa, the MHL species for macropaquin, and the MH_2L species for macroquin–SO_3. These data indicate that the 8-hydroxyquinoline donors retain their basicity when bound to the Ba^{2+} ion. The presence of two such donors in macroquin–SO_3 gives rise to the large prevalence of the protonated complex MH_2L near neutral pH.

In comparing the thermodynamic properties of these ligands to the commonly employed ligands DOTA and DTPA, it is noteworthy that the log K_{BaL} value of 11.11 for macropa is substantially larger than that for DTPA (8.78) and only 0.64 log units lower than that for DOTA, indicating that macropa is a high-affinity ligand for Ba^{2+}. A more accurate reflection of thermodynamic affinity in aqueous solution, however, can be expressed using conditional stability constants, which account for the effect of protonation equilibria of the ligands on complex stability.[43,44] The conditional stability constants (log K′) of the AE complexes at pH 7.4 are given in Table 1. The log K'_{Ba} value of 10.74 for macropa is 5–6 orders of magnitude greater than those for DOTA (5.72) and DTPA (4.63). Macropa also exhibits higher affinity for Ba^{2+} at pH 7.4 than macropaquin (log K′ = 10.05) and macroquin–SO_3 (log K′ = 8.76). From these values, macropa emerges as remarkably superior to all other ligands for the chelation of Ba^{2+} at near-neutral pH.

Another measure of conditional thermodynamic affinity of a ligand for a metal ion is provided by pM values (Table 1), which are defined as the negative log of the free metal concentration in a pH 7.4 solution containing 10^{-6} M metal ion and 10^{-5} M ligand.[45] Larger pM values correspond to higher affinity chelators because they indicate that there is a smaller concentration of free metal ions under these conditions at equilibrium. The pBa values of DOTA and DTPA are only 6.76 and 6.15, respectively, reflecting the presence of a significant amount of free Ba^{2+} at pH 7.4 (Figure 2). By contrast, 90% of Ba^{2+} is already bound by macropa at pH 4.0 and 99% is complexed at pH 5.1, consistent with the high pBa value of 11.69 for this ligand. Furthermore, macropa is 1.17-fold and 1.79-fold more selective for Ba^{2+} over Sr^{2+} and Ca^{2+}, respectively, as determined by the ratio of the corresponding pM values. By contrast, these selectivity values are <1 for DOTA and DTPA, emphasizing their poor affinities for the large Ba^{2+} ion at pH 7.4.

Having demonstrated that macropa chelates Ba^{2+} with high thermodynamic stability and selectivity, the kinetic inertness of this complex was examined in comparison to that of macropaquin and macroquin–SO_3. We first challenged the Ba–L complexes with 1000 equiv of La^{3+}, a metal that forms a complex of high thermodynamic stability with macropa (log K_{LaL} = 14.99).[27] The substitution of Ba^{2+} with La^{3+} was monitored at RT and pH 7.3 by UV-vis spectrophotometry (Figures S27–S29). Ba–macropa and Ba–macropaquin exhibited moderate stability, giving rise to similar half-lives of 5.45 ± 0.20 min and 6.07 ± 0.13 min, respectively. By contrast, Ba–macroquin–SO_3 underwent transmetalation with La^{3+} much more rapidly ($t_{½}$ = 0.65 ± 0.05 min), indicating that macroquin-SO_3 cannot adequately retain Ba^{2+} under these conditions.

Because Ba^{2+} possesses bone-seeking properties, the stability of the Ba^{2+} complexes in the presence of hydroxyapatite ($Ca_5(PO_4)_3(OH)$, HAP), the predominant mineral that comprises bone, was also evaluated.[46,47] HAP was suspended in solutions containing the complexes formed in situ (1.1 equiv L, 1.0 equiv Ba^{2+}) in pH 7.6 buffer, and the amount of Ba^{2+} remaining in the liquid phase, reflecting intact Ba–L complex, was determined by graphite furnace atomic absorption spectroscopy (GFAAS) (Figure S30). Whereas free Ba^{2+} is adsorbed by HAP in less than 10 min, Ba–macropa and Ba–macropaquin respectively retained 82% and 68% of this ion after 20 h. Ba–macroquin–SO_3 displayed the least stability in the presence of HAP, with only 17% of the complex remaining intact after 20 h. Taken together, the results of these challenges demonstrate that Ba–macropa and Ba–macropaquin are considerably more stable than Ba-macroquin–SO_3 under extreme conditions of large excesses of competing metal ions. This feature may be important for Ba^{2+} chelation in industrial applications, such as scale dissolution, because numerous other metal ions are present during these processes. The inferior kinetic stability of Ba–macroquin–SO_3 relative to the other two complexes correlates with the lower thermodynamic affinity of this ligand for Ba^{2+} and is most likely a consequence of the fact that the diprotonated Ba^{2+} complex of macroquin-SO_3, MH_2L, is the major species at pH 7.4 (Figure 2). This complex is expected to be substantially more labile than the ML species due to decreased electrostatic interactions between the ion and ligand.

The encouraging results of the thermodynamic and kinetic stability studies prompted us to evaluate the feasibility of employing macropa and macropaquin as $BaSO_4$ scale dissolvers. First, a suspension of $BaSO_4$ in pH 8 $NaHCO_3$ was formed by combining $Ba(NO_3)_2$ (4.53 mM) with excess Na_2SO_4 (13.48 mM), simulating the mixing of incompatible waters that produces $BaSO_4$ scale in petroleum operations. The resulting $BaSO_4$ suspension was treated with ligand (5 mM), and the amount of dissolved Ba^{2+} was measured by GFAAS (Figure 3). Macropa rapidly solubilized 78% of $BaSO_4$ in just 10 min and afforded complete dissolution after 30 min. Likewise, macropaquin dissolved 95% of $BaSO_4$ in 30 min. By contrast, the conventional ligands DOTA and DTPA dissolved only 40% of $BaSO_4$ within this same time, underscoring the inferior solubilizing properties of these ligands at pH 8.

The dissolution of $BaSO_4$ by macropa, DTPA, and DOTA was further evaluated in pH 11 $NaCO_3$ buffer (Figure S31) to match the caustic conditions that are applied in the industrial setting. Impressively, macropa solubilized >95% of the $BaSO_4$ in just 5 min. DTPA also dissolved nearly all the $BaSO_4$ in this same time. The improved dissolution ability of DTPA at pH 11 versus pH 8 reflects the greater proportion of the fully deprotonated ligand ($DTPA^{5-}$) present at pH 11, which favors Ba–DTPA complex formation. These results are consistent with the fact that the petroleum industry only uses this ligand under conditions of high pH.[16–18] The similar rates at which macropa and DTPA solubilize $BaSO_4$ at pH 11 suggest that macropa possesses remarkably fast Ba^{2+}-binding kinetics. The macrocycle DOTA, by contrast, was unable to completely dissolve all the $BaSO_4$. After 30 min, only 75% dissolution was reached, signifying that the kinetics of metal incorporation for DOTA remain slow even at high pH.

We next investigated the ligand-promoted dissolution of crude barite ore, which is composed predominately of $BaSO_4$, as a model for the solid deposits of natural scale that plague the petroleum industry. Barite rocks (Figure 4a) obtained from Excalibar Minerals (Katy, TX) were milled and sieved to isolate particles between 0.5 and 2 mm (Figure 4b). To simulate production tubing clogged with $BaSO_4$ scale, polypropylene columns were filled with barite (3 g), to which solutions of macropa or DTPA at pH 8 or 11 were added (Figure 4c). The concentration of each ligand solution was approximately 48 mM, consistent with the dilute compositions of scale dissolvers used industrially.[11,13,16,18,48] After a soak time of 1 h, the ligand solution was eluted from the column, and the concentration of dissolved barium was measured by GFAAS and converted to ligand efficiency (Eq. 4).

$$Ligand\ Efficiency = \frac{Ba_{exp}}{Ba_{max}} \times 100 \quad (4)$$

In Eq. 4, Ba_{exp} is the concentration of barium measured in the eluate, and Ba_{max} is the maximum concentration of barium that can be chelated by each ligand, calculated from the concentration of each ligand applied to the column and assuming a 1:1 M:L binding model. As shown in Figure 4d, the ligand efficiency of macropa at pH 8 is 40%, indicating that nearly half of the ligand solution was saturated with Ba^{2+} following exposure to barite for 1 h. DTPA, by contrast, was practically incapable of dissolving barite at this pH, giving rise to a ligand efficiency of only 2%. Macropa remained equally as effective at pH 11, again displaying a ligand efficiency of 40%. By contrast, even at pH 11, the dissolution efficiency of DTPA was only 17%, less than half that observed for macropa. Collectively, these results indicate that macropa maximally dissolves barite at or below pH 8, underscoring its superior affinity for Ba^{2+} near neutral pH.

Lastly, the capacity for recovery and reuse of macropa post-$BaSO_4$ dissolution was assessed qualitatively (Figure 5). A sample of macropa-dissolved $BaSO_4$ (9.66 mM macropa, 8.74 mM $Ba(NO_3)_2$, 26.04 mM Na_2SO_4) was acidified to pH 1 with concentrated HCl to protonate the ligand, inducing Ba^{2+} decomplexation and precipitation as $BaSO_4$. The macropa solution was isolated by filtration, basified to pH 8 with 2 M NaOH, and combined with another portion of $BaSO_4$. Within 40 min, no visible precipitate remained in the vial, signaling that the recycled macropa dissolved all the $BaSO_4$. Subsequently, the ligand was recovered and reused for $BaSO_4$ dissolution four more times with a negligible loss in efficacy or speed of dissolution (Figure S33). These results demonstrate the facile and economic reuse of macropa, an attractive feature that will facilitate its implementation in industry.[49]

Conclusion

In summary, three ligands based on the expanded diaza-18-crown-6 macrocycle were evaluated for their abilities to chelate the large Ba^{2+} ion. Macropa exhibits unprecedented affinity for Ba^{2+} at pH 7.4, possessing a log K′ value of 10.74. The Ba^{2+} complexes of both macropa and macropaquin display substantial kinetic stability when challenged with La^{3+} or HAP, whereas macroquin–SO_3 rapidly releases Ba^{2+} under these conditions. Additionally, macropa and macropaquin can efficiently dissolve $BaSO_4$ under RT and near-neutral pH conditions. This feature was further reflected in dissolution studies involving authentic barite ore samples, which showed macropa to be superior to the state-of-the-art chelator DTPA. The promising Ba^{2+}-chelation properties of this ligand will render it useful for the dissolution of $BaSO_4$ scale deposits, fulfilling an important unmet need in the petroleum industry.

More broadly, these results reveal key features that are required for stable coordination of the heavy AE ions. Namely, the observation that picolinate donors provide superior coordination properties for Ba^{2+} in contrast to 8-hydroxyquinoline donors will guide future ligand design efforts for this underexplored metal ion. These results have further implications in the realm of radiochemistry, where these chelators may be applied for the chelation of Ra^{2+}. Due to both concerns about radiological contamination of ^{226}Ra in NORM and the great therapeutic potential of ^{223}Ra for the treatment of cancer, a better understanding of AE chemistry will advance efforts to chelate Ra^{2+} for these important applications.

Supplementary Material

Refer to Web version on PubMed Central for supplementary material.

ACKNOWLEDGMENTS

The authors thank Dr. Vojtěch Kubíček (Charles University, Prague, The Czech Republic) for his valuable guidance with potentiometry and Excalibar Minerals (Katy, TX) for providing us with a sample of barite ore.

Funding Sources

This work was supported by Cornell University and by a Pilot Award from the Weill Cornell Medical College Clinical and Translational Science Center, funded by NIH/NCATS UL1TR00457. This research made use of the NMR Facility at Cornell University, which is supported in part by the NSF under award number CHE-1531632.

REFERENCES

(1). Beryllium, Magnesium, Calcium, Strontium, Barium and Radium In Chemistry of the Elements, 2nd Ed.; Greenwood N, Earnshaw A, Eds.; Butterworth-Heinemann: Oxford, 1997; pp 107–138.

(2). Shannon RD Acta Crystallogr. Sect. A 1976, 32, 751–767.

(3). Schott GD Med. Hist 1974, 18, 9–21. [PubMed: 4618587]

(4). CRC Handbook of Chemstry and Physics, 87th ed.; Lide DR, Ed.; CRC Press: Boca Raton, 2006.

(5). Li J; Tang M; Ye Z; Chen L; Zhou YJ Dispersion Sci. Technol 2017, 38, 661–670.

(6). Clemmit AF; Ballance DC; Hunton AG The dissolution of scales in oilfield systems. SPE14010/1, presented at SPE, Aberdeen, U.K. 9 10–13, 1985.

(7). Crabtree M; Eslinger D; Fletcher P; Miller M; Johnson A; King G Oilfield Rev. 1999, 11, 30–45.

(8). Zielinski RA; Otton JK Naturally occurring radioactive materials (NORM) in produced water and oil-field equipment—An issue for the energy industry. U.S. Geological Survey Fact Sheet FS–142–99, 9, 1999.

(9). Ghose S; Heaton B In The Natural Radiation Environment VII: VIIth Int. Symp. On the NRE; Radioactivity in the Environment; Elsevier, 2005; Vol. 7, pp 1081–1089.

(10). de Jong F; Reinhoudt DN; Torny-Schutte GJ; van Zon A Novel macrocyclic polyethers and the use of salts thereof for dissolving barium sulfate scale. Brit. UK Pat. Appl GB2024822A, 1 16, 1980.

(11). Lakatos I; Lakatos-Szabó J; Kosztin B Comparative study of different barite dissolvers: Technical and economic aspects. SPE 73719, presented at SPE, Lafayette, LA, U.S.A., 2 20–21, 2002.

(12). Almubarak T; Ng JH; Nasr-El-Din H Oilfield scale removal by chelating agents: An aminopolycarboxylic acids review. SPE-185636-MS, presented at SPE, Bakersfield, CA, 4 23, 2017.

(13). Mason DJ Formulations and methods for mineral scale removal. U.S. Patent Appl US20170369764A1, 12 28, 2017.

(14). Mason DJ Composition for removing naturally occurring radioactive material (NORM) scale. U.S. Patent Appl US20170313927A1, 11 2, 2017.

(15). Martell AE; Smith RM Critical Stability Constants: Vol. 1; Plenum Press: New York; London, 1974.

(16). Putnis A; Putnis CV; Paul JM. The efficiency of a DTPA-based solvent in the dissolution of barium sulfate scale deposits. SPE 29094, presented at SPE, San Antonio, TX, U.S.A. 2 14–17, 1995, 773–785.

(17). Dunn K; Yen TF Environ. Sci. Technol 1999, 33, 2821–2824.

(18). Putnis CV; Kowacz M; Putnis A Appl. Geochem 2008, 23, 2778–2788.

(19). Stetter H; Frank W; Mertens R Tetrahedron 1981, 37, 767–772.

(20). Delgado R; Fraûsto Da Silva JJR Talanta 1982, 29, 815–822. [PubMed: 18963244]

(21). Clarke ET; Martell AE Inorg. Chim. Acta 1991, 190, 27–36.

(22). Wang K-S; Tang Y; Shuler PJ; Dunn KJ; Koel BE; Yen TF Effect of scale dissolvers on barium sulfate deposits: A macroscopic and microscopic study. Paper 02309, presented at NACE, January 1, 2002.

(23). Poonia NS; Bajaj AV Chem. Rev 1979, 79, 389–445.

(24). Thiele NA; Brown V; Kelly JM; Amor-Coarasa A; Jermilova U; MacMillan SN; Nikolopoulou A; Ponnala S; Ramogida CF; Robertson AKH; Rodríguez-Rodríguez C; Schaffer P; Williams C Jr.; Babich JW; Wilson JJ Angew. Chem. Int. Ed 2017, 56, 14712–14717.

(25). Thiele NA; Wilson JJ Cancer Biother. Radiopharm 2018, doi: 10.1089/cbr.2018.2494.

(26). Kelly JM; Amor-Coarasa A; Ponnala S; Nikolopoulou A; Williams C Jr.; Thiele NA; Schlyer D; Wilson JJ; DiMagno SG; Babich JW J. Nucl. Med 2018, Accepted.

(27). Roca-Sabio A; Mato-Iglesias M; Esteban-Gómez D; Tóth É; de Blas A; Platas-Iglesias C; Rodríguez-Blas T J. Am. Chem. Soc 2009, 131, 3331–3341. [PubMed: 19256570]

(28). Jensen MP; Chiarizia R; Shkrob IA; Ulicki JS; Spindler BD; Murphy DJ; Hossain M; Roca-Sabio A; Platas-Iglesias C; de Blas A; Rodríguez-Blas T Inorg. Chem 2014, 53, 6003–6012. [PubMed: 24890863]

(29). Ferreirós-Martínez R; Esteban-Gómez D; Tóth É; de Blas A; Platas-Iglesias C; Rodríguez-Blas T Inorg. Chem 2011, 50, 3772–3784. [PubMed: 21413756]

(30). Su N; Bradshaw JS; Zhang XX; Song H; Savage PB; Xue G; Krakowiak KE; Izatt RM J. Org. Chem 1999, 64, 8855–8861. [PubMed: 11674789]

(31). Zhang XX; Bordunov AV; Bradshaw JS; Dalley NK; Kou X; Izatt RM J. Am. Chem. Soc 1995, 117, 11507–11511.

(32). Bordunov AV; Bradshaw JS; Zhang XX; Dalley NK; Kou X; Izatt RM Inorg. Chem 1996, 35, 7229–7240. [PubMed: 11666912]

(33). Bhavan R; Hancock RD; Wade PW; Boeyens JCA; Dobson SM Inorg. Chim. Acta 1990, 171, 235–238.

(34). Hancock RD; Siddons CJ; Oscarson KA; Reibenspies JM Inorg. Chim. Acta 2004, 357, 723–727.

(35). Jensen KA Inorg. Chem 1970, 9, 1–5.

(36). Boros E; Ferreira CL; Cawthray JF; Price EW; Patrick BO; Wester DW; Adam MJ; Orvig C J. Am. Chem. Soc 2010, 132, 15726–15733. [PubMed: 20958034]

(37). Wang X; De Guadalupe Jaraquemada-Pelaéz M; Cao Y; Pan J; Lin K-S; Patrick BO; Orvig C Inorg. Chem 2018, doi: 10.1021/acs.inorgchem.8b01208.

(38). Hancock RD; Motekaitis RJ; Mashishi J; Cukrowski I; Reibenspies JH; Martell AE J. Chem. Soc., Perkin Trans 2 1996, 1925–1929.

(39). Rohovec J; Kyvala M; Vojtisek P; Hermann P; Lukes I Eur. J. Inorg. Chem 2000, 195–203.

(40). Martell AE; Hancock RD; Motekaitis RJ Coord. Chem. Rev 1994, 133, 39–65.

(41). Doble DMJ; Melchior M; O'Sullivan B; Siering C; Xu J; Pierre VC; Raymond KN Inorg Chem 2003, 42, 4930–4937. [PubMed: 12895117]

(42). Schmitt-Willich H; Brehm M; Ewers CL; Michl G; Müller-Fahrnow A; Petrov O; Platzek J; Radüchel B; Sülzle D Inorg. Chem 1999, 38, 1134–1144. [PubMed: 11670895]

(43). Alberty RA Eur. J. Biochem 1996, 240, 1–14. [PubMed: 8925834]

(44). Burgot JL Conditional Stability Constants In Ionic Equilibria in Analytical Chemistry. Springer, New York, 2012; pp 485–501.

(45). Harris WR; Carrano CJ; Raymond KN J. Am. Chem. Soc 1979, 101, 2722–2727.

(46). Li WP; Ma DS; Higginbotham C; Hoffman T; Cutler CS; Jurisson SS Nucl. Med. Biol 2001, 28, 145–154. [PubMed: 11295425]

(47). Cawthray JF; Creagh AL; Haynes CA; Orvig C Inorg. Chem 2015, 54, 1440–1445. [PubMed: 25594577]

(48). Jordan MM; Williams H; Linares-Samaniego S; Frigo DM New insights on the impact of high temperature conditions (176°C) on carbonate and sulphate scale dissolver performance. SPE-169785, presented at SPE, Aberdeen, U.K., 5 14–15, 2014.

(49). Morris RL; Paul JM Method for regenerating a solvent for scale removal from aqueous systems. PCT Int. Appl WO9206044A1, 4 16, 1992.

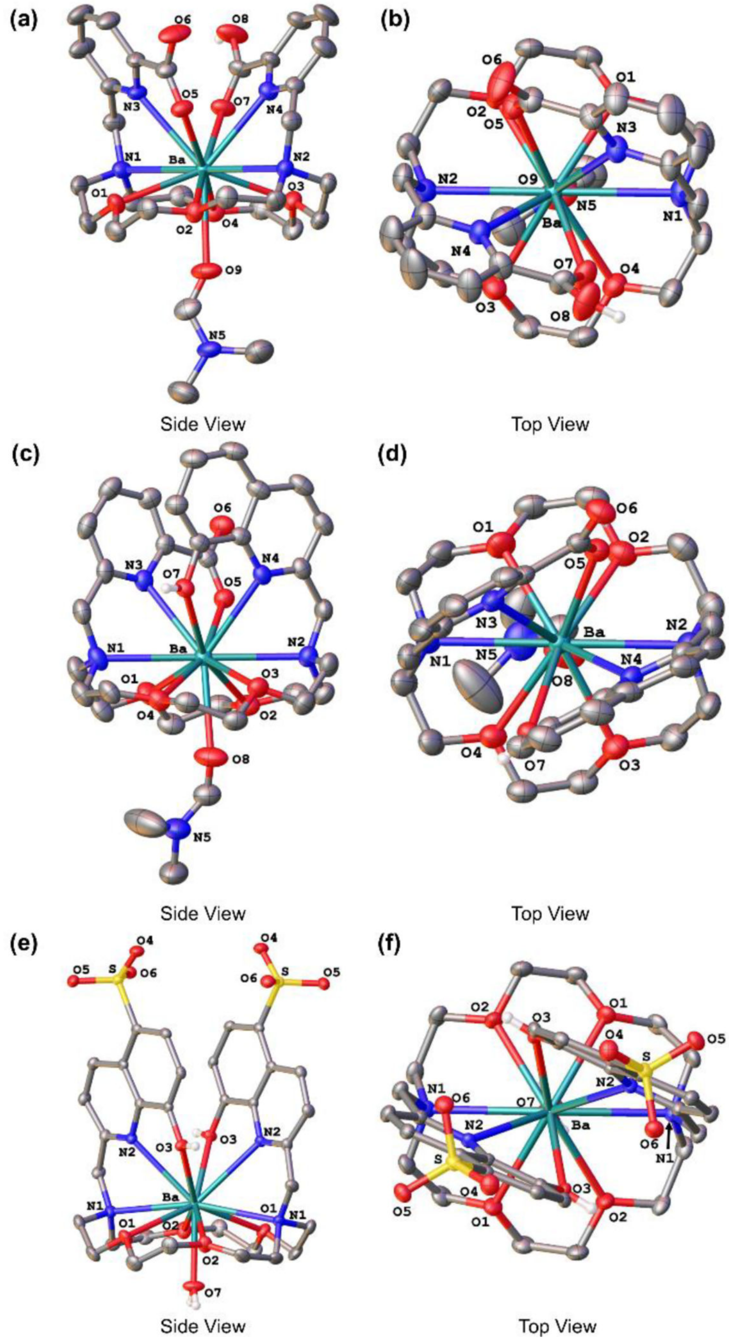

Figure 1.

X-ray crystal structures of [Ba(Hmacropa)(DMF)]ClO_4•Et_2O (a,b), [Ba(Hmacropaquin)(DMF)]ClO_4•DMF (c,d), and [Ba(H_2macroquin–SO_3)(H_2O)]•4H_2O (e,f). Ellipsoids are drawn at the 50% probability level. Counteranions, non-acidic hydrogen atoms, and outer-sphere solvent molecules are omitted for clarity.

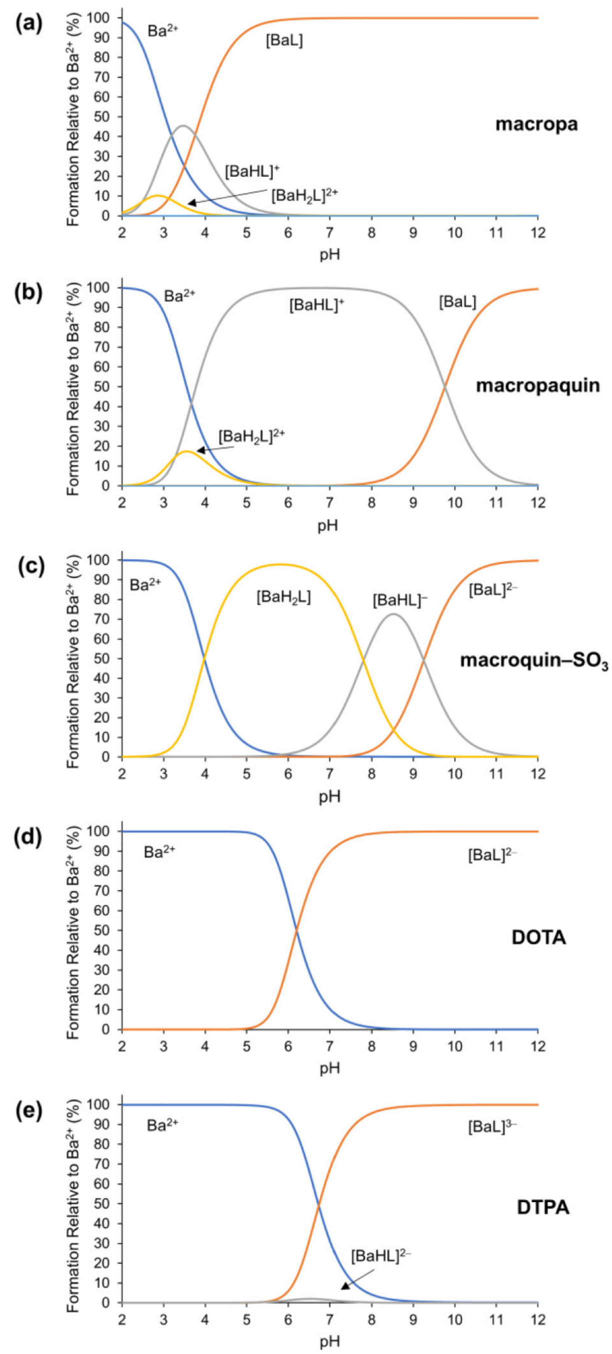

Figure 2.

Species distribution diagrams of (a) macropa, (b) macropaquin, (c) macroquin–SO_3, (d) DOTA, and (e) DTPA in the presence of Ba^{2+} at $[Ba^{2+}]_{tot} = [L]_{tot}$ = 1.0 mM, I = 0.1 M KCl, and 25 °C.

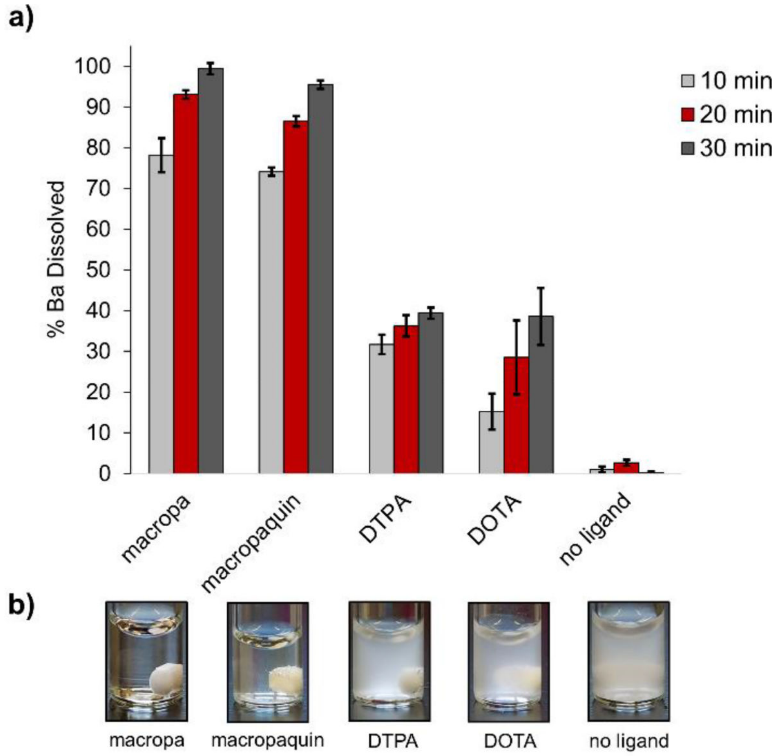

Figure 3.

Dissolution of $BaSO_4$ by macropa, macropaquin, DTPA, and DOTA. (a) Dissolution at RT and pH 8 was initiated by the addition of chelator (5 mM) to a suspension of $BaSO_4$ (4.53 mM $Ba(NO_3)_2$ and 13.48 mM Na_2SO_4). Barium content in solution was measured by GFAAS after 10, 20, and 30 min. (b) Samples from dissolution experiments after 30 min.

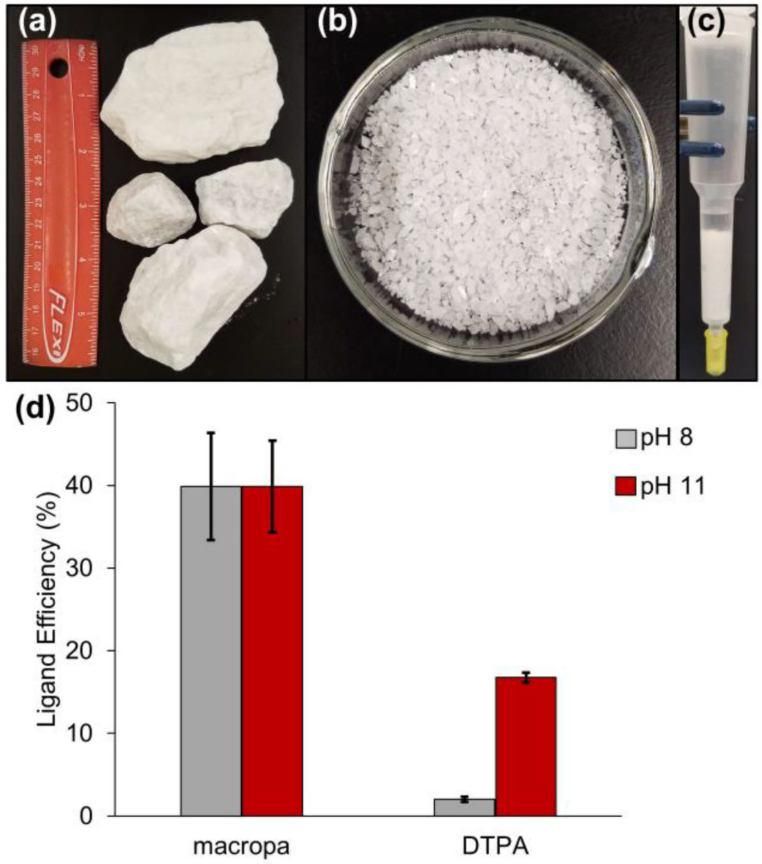

Figure 4.

Barite dissolution efficiency of macropa and DTPA. (a) Large rocks of crude barite ore were crushed with a hammer. (b) The barite was sieved to isolate particles between 0.5 and 2 mm. (c) To simulate petroleum pipes clogged with $BaSO_4$ scale, columns were filled with barite (3 g), and then solutions of macropa or DTPA (~48 mM) at pH 8 and pH 11 were added. (d) After a soak period of 1 h, ligand efficiency, or the percent of ligand saturated with Ba^{2+}, was determined by measuring the concentration of barium in the eluate by GFAAS.

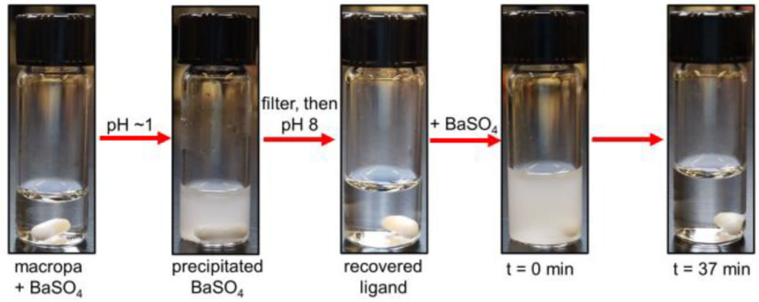

Figure 5.

Ligand recovery and reuse. A solution of macropa-dissolved $BaSO_4$ was acidified to release the Ba^{2+} from the ligand as $BaSO_4$. After filtration of the precipitated $BaSO_4$ and basification of the solution, the recovered ligand was successfully reused for another cycle of $BaSO_4$ dissolution.

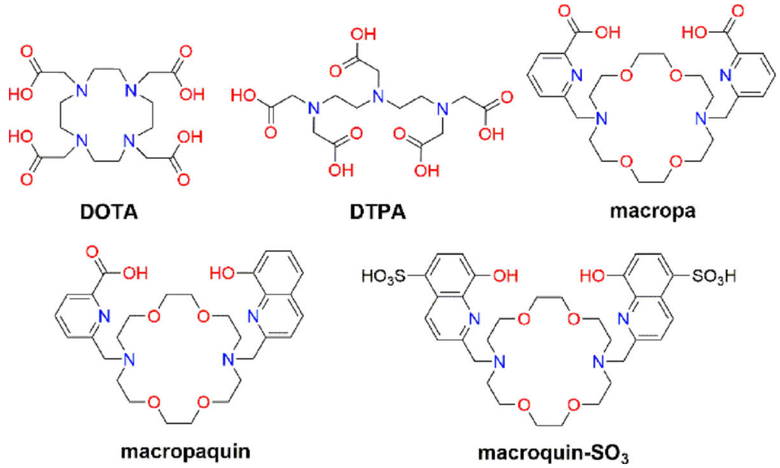

Chart 1.
Structures of the Ligands Discussed in this Work

Table 1.

Protonation Constants of macropa^{2-}, macropaquin^{2-}, and macroquin–SO_3^{4-} and Thermodynamic Stability Constants of Their Alkaline Earth Complexes Determined by pH-Potentiometry (25 °C and I = 0.1 M KCl).[a]

	macropa^{2-}	macropaquin^{2-}	macroquin–SO_3^{4-}	DOTA^{4-} [b]	DTPA^{5-} [c]
log K_{a1}	7.41(1) (7.41)[d]	10.33(4)	9.34(4)	11.14	10.34
log K_{a2}	6.899(3) (6.85)	7.15(3)	9.43(1)	9.69	8.59
log K_{a3}	3.23(1) (3.32)	6.97(2)	6.75(4)	4.85	4.25
log K_{a4}	2.45(5) (2.36)	3.24(4)	6.62(4)	3.95	2.71
log K_{a5}	(1.69)				2.18
log K_{CaL}	5.79(1) [5.25][e]	5.90(4)	6.04(8)	16.37	11.77
log K_{CaHL}		8.59(2)	8.60(4)	3.60	6.10
log K_{SrL}	9.442(4) [9.57]	9.19(5)	8.62(2)	14.38	9.68
log K_{SrHL}	3.35(8) [4.16]	8.92(2)	8.34(4)	4.52	5.4
log K_{SrH2L}			6.920(3)		
log K_{BaL}	11.11(4)	10.87(2)	10.44(6)	11.75	8.78
log K_{BaHL}	3.76(2)	9.76(2)	9.24(7)		5.34
log K_{BaH2L}	2.49(7)	3.28(2)	7.80(2)		
log K'_{Ca} [f]	5.42	3.94	3.19	10.34	7.63
log K'_{Sr} [f]	9.07	7.54	5.64	8.35	5.53
log K'_{Ba} [f]	10.74	10.05	8.76	5.72	4.63
pCa[g]	6.54	6.04	6.01	11.29	8.59
pSr[g]	10.02	8.50	6.70	9.30	6.61
pBa[g]	11.69	11.01	9.72	6.76	6.15

[a]Data reported previously for DOTA^{4-} and DTPA^{5-} are provided for comparison.

[b]Ref 21, I = 0.1 M KCl.

[c]Protonation constants and log K_{CaL} from Ref 42, I = 0.1 M KCl. Other values from Ref 15.

[d]Parenthetic values from Ref 27, I = 0.1 M KCl.

[e]Bracketed values from Ref 29, I = 0.1 M KNO_3.

[f]Conditional stability constant at pH 7.4, 25 °C, and I = 0.1 M KCl.

[g]Calculated from $-\log [M^{2+}]_{free}$ ($[M^{2+}] = 10^{-6}$ M; $[L] = 10^{-5}$ M; pH 7.4; 25 °C; I = 0.1 M KCl).